Review

A Review on Recent Advancements of Graphene and Graphene-Related Materials in Biological Applications

Federica Catania [1], Elena Marras [1], Mauro Giorcelli [2,3], Pravin Jagdale [2], Luca Lavagna [1,3], Alberto Tagliaferro [1,2,4] and Mattia Bartoli [1,3,*]

1   Department of Applied Science and Technology, Politecnico di Torino, C. so Duca degli Abruzzi 24, 10129 Torino, Italy; federica.catania@studenti.polito.it (F.C.); elena.marras@studenti.polito.it (E.M.); luca.lavagna@polito.it (L.L.); alberto.tagliaferro@polito.it (A.T.)
2   Italian Institute of Technology, Via Livorno 60, 10144 Torino, Italy; mauro.giorcelli@polito.it (M.G.); pravin.jagdale@iit.it (P.J.)
3   Consorzio Interuniversitario Nazionale per la Scienza e Tecnologia dei Materiali (INSTM), Via G. Giusti 9, 50121 Florence, Italy
4   Faculty of Science, Ontario Tech University, 2000 Simcoe Street North, Oshawa, ON L1G 0C5 T, Canada
*   Correspondence: mattia.bartoli@polito.it; Tel.: +39-011097348

Abstract: Graphene is the most outstanding material among the new nanostructured carbonaceous species discovered and produced. Graphene's astonishing properties (i.e., electronic conductivity, mechanical robustness, large surface area) have led to a deep change in the material science field. In this review, after a brief overview of the main characteristics of graphene and related materials, we present an extensive overview of the most recent achievements in biological uses of graphene and related materials.

Keywords: graphene; graphene oxide; biomaterials; drug delivery

1. Introduction

In recent years, nanoscale technologies have become the last frontier in material science and pharmaceutical development [1]. A primary role has been played in this by nanostructured carbonaceous materials [2,3] such as carbon nanotubes and graphene (GF) due to their intrinsic properties and easy functionalization [4].

Nowadays, graphene and related materials represent the most advanced frontier in high-performance carbon materials [5] as witnessed by the European Union research council enforcing a strong action named EU Graphene Flagship [6]. This plan aimed to promote basic investigation on graphene and its related derivatives in order to establish the European Community as a world leader in the field [5]. This was consequent to the top properties of this allotropic one-atom-thick planar sheet of carbon tightly packed into a hexagonal cell structure [7]. Graphene and its related materials' features can be exploited in a wide range of applications to improve the mechanical robustness and electronic properties of composite materials [8–10], both plastics [11,12] and metals [13,14], even at a very limited amount However, its price is not negligible, hindering its way through to the market with respect to cheaper solutions [15–23]. Due their high cost, graphene and related materials cannot be used in cheap, large-scale production. However, they can be employed in high-added-cost applications such as those represented by frontier medicine [24].

This field has been boosted up by vicious diseases and the increased concern for human healthiness. Pharmaceutical companies and academic institutions have deeply committed themselves to drive to unreached levels newly designed drugs and procedures [25,26]. Despite the wide numbers of available established protocols, new routes [27,28] are explored to develop new and innovative materials for drug delivery [29], regenerative medicine [30], theragnostic treatment [31], and tissue repairing [32].

Furthermore, the development of new antimicrobial agents has become a primary interest to contrast the increase of antibiotic resistance in the bacterial world [33].

All these issues have been deeply investigated by nanoscience and material technology. Graphene and related materials could represent a ground-breaking event for facing all the above-mentioned issues due to the tunability, biocompatibility, and physiochemical properties. Accordingly, in this review, we present the most recent advancements achieved by using graphene and its related materials for biological applications ranging from biomaterials to drug delivery and theragnostics.

2. Graphene and Graphene-Related Materials

2.1. Overview on Graphene and Related Materials

Graphene is ideally a single plane of graphite with no defect sites. Carbon atoms of the graphene elementary cell are bonded through three σ bonds with the p orbitals perpendicular to the sp^2 plane. This structure allows the total delocalization of the π bond on the graphene plane. Consequently, the π-electrons freely move alongside the graphene plane [34–36]. This is the reason of its high electrical conductivity and carrier rate [37].

The astonishing properties of neat graphene are counterbalanced by the difficulties in handling it and by its scarce availability [38]. As a matter of fact, plenty of literature uses the term graphene to define nanographite and a few layered materials [39,40]. In order to overcome the issues related to the use of real neat graphene, several materials have been proposed. The first alternative is graphene oxide (GO). GO is an oxidized graphene derivative rich in oxygen functionalities [41]. The main residual groups on the GO basal lattice are epoxide and hydroxyl groups, while carbonyl and carboxylic ones are more abundant on the edges. Contrary to pure neat graphene, GO's structure is deeply affected by its preparation methodologies.

The production of GO started more than fifteen decades ago with the chemical reactivity of graphite studied by Brodie in 1859 during the measurements to identify the atomic weight of carbon [42]. In his experiments, Brodie oxidized graphite by using a mixture of nitric acid and potassium chlorate for long times, up to days. He obtained a light-yellow powder characterized by brilliant transparent flakes. Brodie called it graphitic acid, but nowadays that material is known as GO. Fifty years later, Staudenmaier reported another methodology for the production of "graphitic acids" by using a highly acidic solution of $KClO_3$ [43]. A further approach was reported by Hummers and Offeman in the mid-twentieth century [44]. In this case, graphite was treated with a sulphuric acid solution of potassium permanganate and sodium nitrate. Nowadays, Hummers' methods is mostly used to produce graphite oxide in laboratories all around the world. Nonetheless, all three methods are still used to produce GO with different features. An exhaustive study was conducted by Poh and co-workers [45] by describing the different properties of reduced GO (rGO) obtained from GO. The authors clearly explain the effect of different oxygen-containing functionalities on the final properties of rGO itself due to the different production methods.

Since different methods are used to synthesize GO, its composition and non-stoichiometric structure are highly based on the production details [46]. Consequently, numerous studies have proposed several structures for GO, namely the Hofmann, Ruess, Scholz–Boehm, Nakajima–Matsuo, Lerf–Klinowski, and Szabo models [47], as shown in Figure 1b–g.
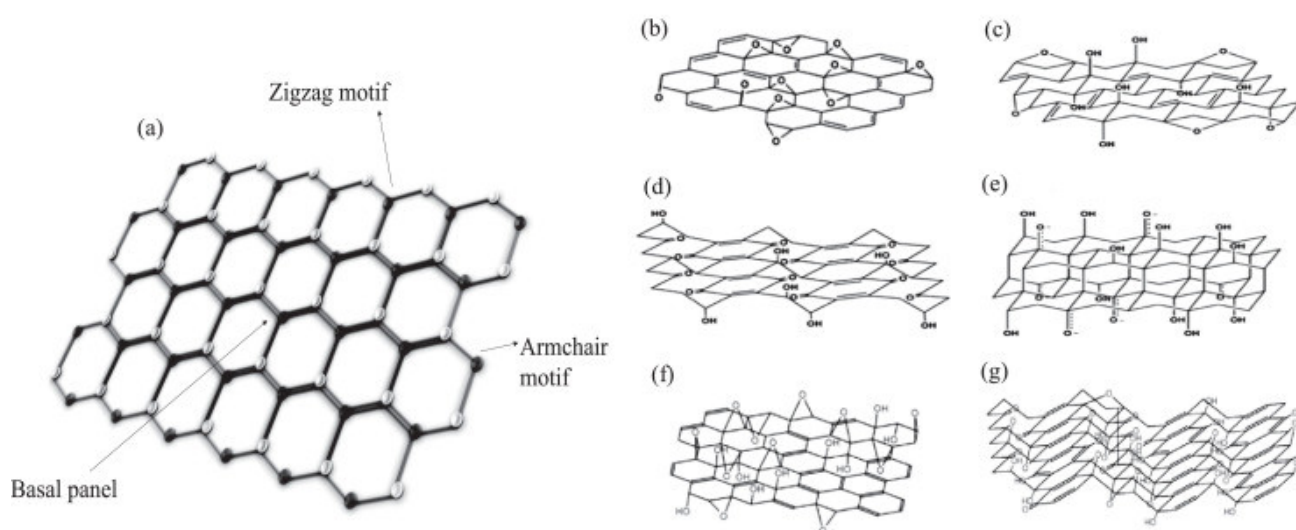
Figure 1. Structures of pristine graphene (**a**) and its GO derivatives based on Hofmann (**b**), Ruess (**c**), Scholz–Boehm (**d**), Nakajima–Matsuo (**e**), Lerf–Klinowski (**f**), and Szabo (**g**) models. Reproduced, adapted, and reprinted with permission from Ref. [48] under CC license.

The scientific community generally agreed on the Lerf–Klinowski as the more realistic structure to describe GO as proved by a plethora of evidences [49]. Based on this model, defects such as cracks, wrinkles, holes, and impurities are principally due to the oxidation process.

GO is not the only graphene derivative that attracted the scientists' attention. The above mentioned rGO is the rising star in the field of graphene research [50].

rGO is produced through a reduction process of GO by using several reductive agents [51,52]. Through reductive process, the oxygenated functional groups of GO are eliminated to form rGO with a carbon to oxygen (C/O) ratio in the range from 12.5 to 0.4 wt.% [53]. Due to their high surface area and stability, they represent the new generation of nanostructured carbon support for plenty of catalytic applications.

The production of new materials by using graphene and graphene-derived materials could be performed by using several approaches based on targeted application.

Graphene and few-layer graphene films could be produced by chemical vapour deposition [54], achieving high-quality materials. However, this approach is limited by the high temperature required, and it is not compatible with all substrates. Alternatively, the spin coating procedure could represent a solid approach to coat any kind of matrix ranging from polymers [55] to inorganic surfaces [56]. Moving to solvent-based approaches, solvent casting could be used to deposit graphene suspensions [57] with a simplified route compared to spin coating but without reaching the same control on deposition. Nonetheless, this approach allows the use of watery GO suspensions, leading to a very facile workability.

Contrary to films, bulk composites were produced by the dispersion of graphene and graphene derivatives in a polymer–metal matrix by using ultrasonication [58] or classical extrusion procedures [59,60].

2.2. Graphene and Related Materials, Characterization

It is important to use the most appropriate characterization technique to evaluate the quality of graphene and the quantity of oxygen on the surface of GO and rGO.

2.2.1. Spectroscopical Techniques

Several spectroscopical techniques have been used to investigate the main features of graphene and related materials.

Raman spectroscopy is a non-destructive technique that allows researchers to evaluate the lattice defectivity of the graphene plates' structure. The Raman spectrum is reported as

the intensity of the signal (arbitrary units) vs. Raman shift (cm^{-1}). The fingerprint of sp2 carbon structures such as graphene is the presence of the D-band at around 1350 cm^{-1}, arising from the disorder-induced phonon mode (A1g-band); the G-band at around 1590 cm^{-1}, assigned to the Raman-allowed phonon mode (E2g-band) [61]; and the 2D band at circa 2700 cm^{-1}. The 2D band is at almost double the frequency of the D-band and originates from second-order Raman scattering process. The extent of the lattice defectivity can be evaluated by the ratio of the intensities of D-band over G-band (I_D/I_G) [62]. The higher the ratio, the greater the amount of lattice defects. The quality and number of graphene layers can be further investigated using Raman spectroscopy.

UV–visible spectroscopy could also be a powerful tool to investigate graphene. Pristine graphene and single-layer graphene oxide (GO) show absorption at 262 and 230 nm respectively in the UV–visible spectrum. This is due to the π–π* transitions of aromatic C–C bonds. Nonetheless, graphene has less transparency than GO, which is attributed to the recovery of sp^2 carbons to restore electronic conjugation in reduced graphene after reduction [63]. Moreover, the transmittance of monolayer graphene is 97.1% at a wavelength of 550 nm, which is higher than that of stacked graphene, as reported by Sun et al. [64]. With the increase in the number of graphene layers, the transmittance of graphene decreased from 94.3% of that of bilayer graphene to 83% of that of six-layer graphene at the same wavelength. Thus, the number of non-defective graphene layers can be determined using UV–visible spectroscopy.

X-ray photoelectron spectroscopy is a surface-sensitive quantitative spectroscopic technique that measures the elemental composition, the chemical state, and the electronic state of the elements that exist within a material [65]. XPS is very useful to investigate graphene and GO because the technique shows what elements are present in the sample and how they are bonded, allowing structural investigation on the material surface [66,67]. XPS technique can give crucial information about the functionalization of graphene and its related materials by the analysis of the C1s peak in the region from 284.1 [68] to 289.4 eV [69]. The decomposition of the C1s peak could be used to identify and quantify the relative ratio of carbon bond types. Furthermore, the presence of a π−π* component at 290.5 eV could be diagnostic to discriminate rGO/graphene from GO that does not show it [70].

2.2.2. X-Ray Diffraction (XRD)

XRD can be one of the tools for the identification of single-layer graphene, with some limitations. Pristine graphite shows a basal reflection (0 0 2) peak at $2\theta = 26.6°$ in the XRD pattern. After pristine graphite is oxidized, the (0 0 2) peak shifts to $2\theta = 13.9°$ due to the existence of an oxygen-functionalized group and water molecules in between the layer of graphite. After GO was completely thermally exfoliated, there was no apparent diffraction peak detected, which means the GO structure was removed and graphene nanosheets were formed [71].

2.2.3. Advanced Microscopic Techniques

Microscopic techniques are necessary to achieve proper characterization of a graphene-related material or composite.

Few-layer graphene flakes can be successfully investigated using atomic force microscopy (AFM) due to a thickness in the range of 0.34–1.2 nm [71,72]. However, this technique cannot be routinely used to scan large areas. In addition, AFM imaging provides topographic images only, which are unable to distinguish the number of layers for GO. However, pristine graphene and GO can be distinguished based on the different thicknesses using AFM imaging. Besides thickness and imaging characterization, different AFM modes can be used to study the mechanical [73], frictional, electrical, magnetic, and elastic properties of graphene nanosheets.

A scanning electron microscope is a type of electron microscope that produces images and analyses the elemental composition (SEM-EDX) of a sample by scanning the surface with a focused beam of electrons. The electrons interact with atoms in the sam-

ple, producing various signals that contain information about the surface topography and the composition of the sample. This technique is mostly used for the morphological characterization.

Transmission electron microscopy is a microscopy technique in which a beam of electrons is transmitted through a specimen to form a see-through image. The specimen is usually either an ultrathin section of the sample (less than 10 nm thick) or a suspension on a grid. The resolving power (the minimum distance between two points for which they can be distinguished as such and not as one) is about 0.2 nm, that is about 20 times greater than the best SEM. Energy dispersive X-ray (EDX) spectra can also be collected to provide information about the elements existing in the samples [74]. It is possible to observe the metal catalyst trapped inside the lattice structure of graphene, and in some cases, it is also possible to distinguish functional groups anchored onto the surface of GO. This technique is used for the morphological characterization of grapheme [75].

2.2.4. Thermogravimetric Analysis (TGA)

Thermogravimetric analysis or thermal gravimetric analysis is an analytical technique used to determine the thermal stability of a material and its fraction of volatile components by monitoring the change in weight that occurs as a specimen is heated [76,77]. The measurement is normally conducted in air or in inert atmosphere, such as helium or argon, and the weight is recorded as a function of increasing temperature. This technique can be coupled to a mass or infrared spectrophotometer to analyse the gases released during the thermal decomposition. TGA is mainly used in the study of the thermal stability of graphene and differences in the thermal degradation between GO and rGO can be distinguished.

3. Graphene and Graphene-Related Materials for Biological Applications

In the following section, we report some of the recent advancements in the use of graphene and related materials for drug delivery, tissue engineering, and regenerative medicine. We start with a brief recap of the advantages and disadvantages of these materials for biological applications in Table 1.

Table 1. Main advantages and disadvantages of graphene and related materials for biological applications.

	Advantages	Disadvantages
Graphene	■ High electrical and thermal conductivities ■ High control on functionalization	■ Hydrophobicity ■ High cost ■ Difficult workability ■ Small production
GO	■ Water dispersibility ■ Polar functionalization ■ Low cost ■ Easy workability	■ Lower electrical and thermal conductivity ■ Surface random functionalization ■ Poor control on post-preparation functionalization
rGO	■ High electrical and thermal conductivities ■ Good control on functionalization ■ Less expensive than neat graphene	■ Hydrophobicity ■ Difficult workability ■ Properties related to production methodology used

3.1. Interaction between Graphene and Related Materials and Biological Systems

Graphene-like materials' viability for biological applications is strongly related to the interactions between graphene and cellular and tissue structures.

Despite the astonishing properties, the use of graphene flakes and rGO as drug carriers without any modification is quite challenging in biological environments due to their high hydrophobicity [78]. The use of GO overcomes this issue due to its high hydrophilicity. This property leads to a cellular uptake through both endocytotic and macro-pinocytotic mechanisms [79,80].

Nonetheless, the use of graphene flakes and rGO in biological environments could be exploited by performing covalent and non-covalent modifications [81]. These less invasive and controlled modifications preserve the high conductivity of graphene flakes and rGO allowing their use in neuronal repairing [82], in vivo cellular imaging [83], and stimuli-mediated drug delivery [84,85].

The extended sp^2 system of graphene and rGO represents a strong advantage with respect to other platforms used in the biological environment such as inorganic nanoparticles [86] due to their facile modifications through cycloadditions [87], e.g., 1,3-dipolar cycloadditions [88], nitrene addition [89], and amide condensation [90]. The intrinsic reactivity of graphene and related materials allows to easily build up compound libraries filled with plenty of materials with the basic properties of graphene and tuned biological activity.

3.2. Graphene and Related Materials as Drug Delivery Platforms

The most investigated biological application of graphene and related materials' still remains drug delivery [91]. The ability of materials to drag and drop chemicals in the human body environment is well exploited by graphene and graphene-related materials [81].

Zhang et al. [92] described the interactions between graphene and proteins elucidating the ability of graphene-based materials to trigger several protein complexes on the cellular membrane to facilitate uptake. This was due to both electron transfer and residual functionalities on graphene-like materials' surface. Wang et al. [93] deeply explored the relationship between graphene's surface topological defects and its ability of drug delivery, proving a strong effect of topology. The authors described the folding ability of these materials in several shapes ranging from nanoscrolls to polyhedral ones. This protean ability allows different interactions with different folding agents such as membrane proteins or nucleic acids. A further study by Mohammed et al. [94] theoretically clarified the loading ability of pristine and metal-decorated graphene materials. Among them, hydrogel and foam are the most attracting solutions because drug release could be triggered by both chemical and thermal modifications [95].

Ezzati et al. [96] produced a biocompatible graphene foam surface tailored with alanine, cysteine, and glycine for cisplatin drug and release. The authors tested the material with a high load of cisplatin on MCF-7 and HepG2 human cancer cell lines with good results. Additionally, the graphene-based carrier underwent biodegradation inside the body according to the mechanism reported in Figure 2.
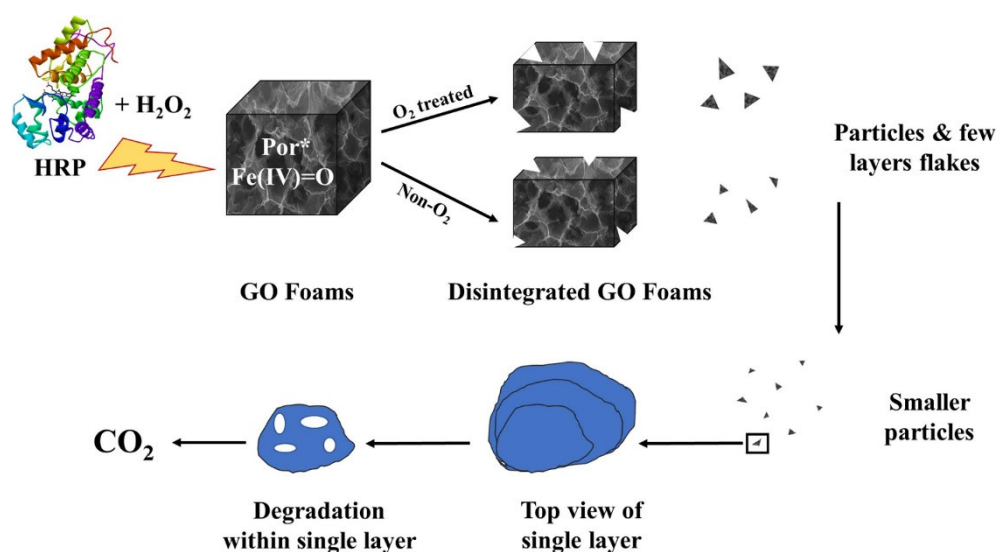
Figure 2. Biodegradation of cisplatin-loaded graphene foams as reported by Ezzati et al. [96].

Authors clearly described that after cellular death the graphene foam was degraded by both reactive oxygen radicals and hydrolytic enzymes. Furthermore, the degradation pathway lead to the formation of carbon dioxide without highly toxic metabolites.

Abdel-Bary et al. [97] studied the release of cisplatin in a very complex graphene-based system containing chitosan, magnetite, and silicon dioxide. By a combination of empirical studies and density functional theory calculation, authors showed that the presence of graphene improved the releasing potentiality up to 91% compared with the other samples tested.

Graphene and related materials also represent a very promising platform for drug release upon biological stimuli, as reported by Trusek et al. [98] in the case of doxorubicin.

Doxorubicin is a widely diffused anticancer drug acting on the S phase of the cellular metabolic pathway [99]. Several studies reveal the efficacy of graphene-based materials as carriers for doxorubicin as reported by Shen et al. [100]. Contrary to polymer-based formulations, graphene and graphene-like materials could act not merely as delivery systems but also as smart platforms to target and release doxorubicin upon several stimuli on a large time window and to monitor the cell vitality [101]. Furthermore, graphene-like materials could be also coupled with polymers to enhance classical formulation effects. The authors proved the effectiveness of chitosan-tailored graphene materials as carriers through molecular dynamic calculation. Doxorubicin interacts with both the π orbital system of graphene and the polar functionalities of the chitosan. After reaching the target, doxorubicin interacts with protein amine and carboxylic residues losing the chitosan interactions. In this case, the weak interactions with the graphene surface are not sufficient, and it was efficiently released.

This effect was magnified considering that the base of the drug delivery systems is the pH release mechanism [102].

Anirudhan et al. [103] described a pH-responsive, GO-based functionalized chitosan nanocomposite for doxorubicin delivery. This system was tailored with folic acid and chitosan through dicyclohexylcarbodiimide coupling using ethyleneglycol dimethacrylate as the cross-linker and potassium peroxydisulphate as an initiator to generate carboxylates able to react with chitosan. The authors loaded the drug by π–π stacking interactions, reporting a loading capacity of up to 95% and a high release rate at pH 5.3. This was particularly attractive for cancerous cell lines with an acidic microenvironment such as L929, HeLa, and MCF7. In vitro tests showed promising results in decrementing their proliferation. Similarly, Omidi et al. [104] developed an innovative pH-sensitive, injectable hydrogel composed by combining chitosan, GO, and cellulose nanowhiskers for the co-delivery of doxorubicin and curcumin that was also studied by Pourjavadi et al. [105].

Authors combined GO with hyperbranched polyglycerol and grafted it with chlorine-based and hydrazine pendants. In this study, doxorubicin was loaded onto the graphene-based carrier by covalent bonding with the hydrazine pendant group, and curcumin was loaded through π–π stacking with GO sheets. The authors claimed a superior biocompatibility together with an improvement of drug internalization. Alipour et al. [106] described an interesting material based on ZnO/dopamine-tailored GO for the enhanced delivery of doxorubicin. The authors evaluated the cytotoxicity of the graphene-based nanohybrid against T47D and MCF10A cellular lines showing a good efficacy together with an antimicrobial activity against Gram-positive and -negative bacteria.

Sattari et al. [107] extended the graphene co-delivery systems' application by the conjugation of GO with cyclodextrins and chitosan fibres for the production of a multidrug loading system. The authors loaded gallic acid and curcumin showing anti-cancer, antimicrobial, antioxidant, and anti-inflammatory activities, which was quite challenging in the absence of graphene-like materials, requiring sophisticated encapsuling procedures [108]. As an alternative to co-delivering, the modification of graphene materials could be a solid choice to enhance the anticancer activity. Jahanshahi et al. [109] produced a highly fluorinated graphene by treating a graphene precursor in an acidic ionic liquid showing a 20% improvement of curcumin loading without compromising the release efficiency. Similarly, Razaghi et al. [110] synthesized fluorinated GO nanosheets able to deliver linoleic–curcumin conjugate and useful for T_2-weighted magnetic resonance imaging. The authors showed that accumulation in the MCF-7 cell line was strictly dependent on pH, and the effectiveness increased moving on to MCF-10A line. Additionally, the authors estimated the relaxation rate as 67.12 $(smM)^{-1}$ and with the very attracting ability to reduce signal intensity in the presence of MCF10A and MCF-7 cells. In vivo studies showed a tumour cell suppression using 4T1 cell line. Zaboli et al. [111] functionalized GO with dopamine altering the surface properties of GO and improving the drug-ability of cytarabine. This tailoring process was modelled by using the DFT approach showing the relevance of orbital interaction during the overall drug loading and release process.

Injectable formulations of graphene-related materials are not the only approach to drug delivery. Li et al. [112] produced a membrane based on GO and Pluronic® F127 for the transdermal delivery of ondansetron. The authors produced a hydrogel with good mechanical properties for topical application, suggesting that the drug flux proportionally decreased with the increase in the level of GO in the hydrogel due to π–π stacking interaction decrement. This meant that the drug release rate can be tuned by tuning the amount of GO as clearly showed by bioavailability tests run on rat models. A GO membrane was also used by Shahabi et al. [113] for delivering tegafur. Molecular dynamics simulation confirmed the strong interaction between GO and drug as mentioned before due to both weak interactions and hydrogen bonds.

Moving forward, graphene and its related materials could be used to drag and drop antibiotics and antimicrobial agents. Abdoli et al. [114] combined poly(vinyl alcohol), tragacanth gum, and GO composite nanofibre for tetracycline delivery, preserving the activity of the antibiotic and controlling the release in time. Authors tested the cytotoxicity against HUVECs as well as agar disk diffusion to determine the antibacterial activity. The cytotoxicity assay showed a high cell viability while antibacterial activity was interestingly high. The buccal administration of clotrimazole though a GO-based formulation was reported by Huang et al. [115]. The authors reported an increased clotrimazole release from the GO films in vitro at up to pH 6.8. Furthermore, they reported an increased activity against *Candida albicans*.

GO-based systems were also used for the delivery of ketamine [116], ibuprofen [117], and medicine for hormone therapy [118]. In all cases, the high control on drug release prevented the sudden increment of drugs, leading to a time-prolonged release.

3.3. Graphene and Related Materials as Tool for Regenerative Medicine and Tissue Repair

The combination of graphene and graphene derivatives with plenty of different matrices has represented a game changing event in the production of biomaterials [119,120]. Fixing or replacing both tissues and organs has been boosted by the graphene-based composites by combining biocompatible scaffolds due to a variety of surface interactions [121].

Tissue engineering is one of the frontiers of medicine, aiming to overcome the drawbacks of the classical transplant procedure through the production of hybrid materials able to perform the same activity as the tissues replaced [122]. Graphene and its related materials have shown very attractive results related to the production of polymeric composites with great mechanical performances together with high biocompatibility for several applications ranging from bone to soft tissue repair [123].

Bahrami et al. [124] combined polyurethane with graphene for the production of conducting-polymer-based-material tissue regeneration. The authors aimed to grow L929 fibroblast and blood vessel endothelial cells on a membrane containing graphene flakes. This was particularly interesting in the case of endothelial cells. Indeed, they could be grown on the inner surface of tubular scaffolds by mimicking the native blood vessel structure [74]. The authors proved the ability of composites to support the attachment, spreading, and proliferation of cell lines. A very close approach was used by Pant et al. [125] for the production of coated stents by using graphene oxide mixed with polyurethane.

As shown in Figure 3, graphene-oxide-based composites create a stable coating on the surface of the stent without any tearing or ablation phenomenon.
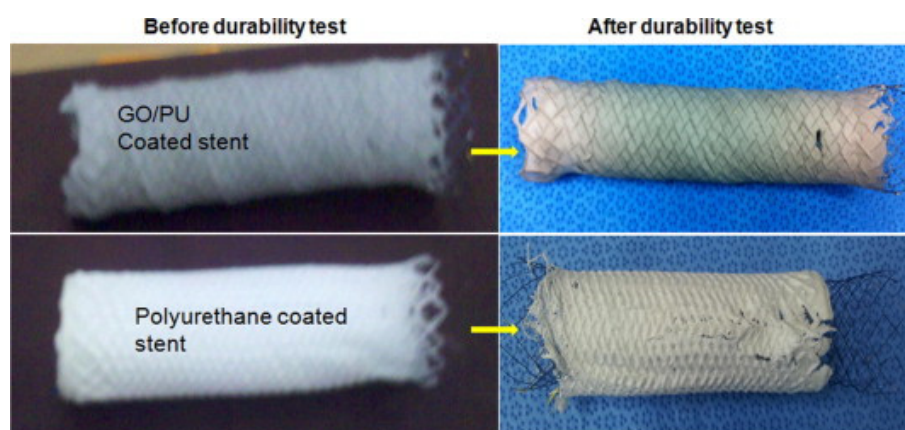

Figure 3. Caption of polyurethane and graphene-oxide-based polyurethane (GO/PU) membrane before and after the coated stent durability test, as reported by Pant et al. [125].

The modification of interphase properties due to the presence of graphene clearly increased the durability of the stent due to the radical-scavenging effect, which preserves the polymeric matrix from degradation promoted by extracellular fluids.

Similar results could be achieved by using titanium-based materials [126], which however show the critical drawback of cellular morphology alteration.

Pathmanapan et al. [127] dispersed graphene oxide into fibrin hydrogel as scaffolds for bone repair proving an enhanced level of biocompatibility, alkaline phosphatase activity, and calcium deposits. This was particularly interesting due the difficulty of solid bone repairing by using polymeric composites and could lead the way to avoid the use of metal alloys [128], preventing the vicious effects related to metal release [129].

Khalili et al. [130] studied the use of an electroactive poly (p-phenylene sulphide) /chitosan mixed with rGO as a potential candidate for tissue engineering. These authors found that high biocompatibility was reached by using an rGO loading of up to 10 wt.% proving a cell attachment and a general porosity of up to 80%. Chitosan was also used in combination with GO and calcium silicate to produce a hierarchical microstructured biomaterial for wound dressing [131]. The authors aimed to reproduce the orderly, porous,

lamellar micron-scale structure of a healing wound, producing a material acting as wound dressing. It was also able to induce photothermal antibacterial and antitumour activity together with wound healing. Wang et al. [132] moved a step forward and combined GO with silk's proteinaceous structure. Silk fibroin materials embedding GO showed an improvement of both mechanical and thermal properties of silk biomaterials, reaching a Young's modulus of up to 1.65 GPa by using only 0.5 wt.% of filler. By in vivo studies, authors showed the improved cell adhesion, growth, and proliferation of fibroblast cells. Graphene and its related materials have boosted the use of poly(lactic acid) (PLA) as matrix for bone repair and tissue engineering [133]. Marques et al. [134] combined PLA with GO and hydroxyapatite for the production of a high hardness and storage modulus, showing an efficient load transfer between the fillers and the polymeric matrix. These results outperformed those achieved by simply using polyglicolides stereocomplexes [135,136] and inorganic composites [137]. Furthermore, PLA/poly(caprolactone) (PCL) blends have been used by Chiesa et al. [138] for the preparation of electrospun fibres with high biocompatibility and a compatible morphology with bone engineering. Poly(ethylene) is another solid solution for the production of biomaterials containing graphene and related materials. Lahiri et al. [139] dispersed graphene nanoplatelets into ultrahigh-molecular-weight poly(ethylene) for orthopaedic implants by using an electrostatic spraying technique. The authors reported that a graphene concentration of up to 0.1 wt.% induced an improvement of fracture toughness of up to 54% and tensile strength increment of up to 71%, while a filler concentration of 1 wt.% increased the elastic modulus and yield strength with a significant decrement of all other properties. The cytotoxicity of graphene nanoplates to osteoblasts was tested, and the authors showed that it is dependent on concentration and graphene agglomeration. Osteoblasts' survival decreased by up to 86% by using composites loaded with 1 wt.% filler, while composites with only 0.1 wt.% of graphene showed a survival reduction of only 16%.

Similarly, Upadhyay et al. [140] studied high-density PE with GO by melt mixing, followed by compression moulding. The uniform dispersion achieved was a key point for the biocompatibility as mentioned before, and the authors achieved an optimum GO dispersion by immobilizing them on the PE surface through nucleophilic addition–elimination reaction. Authors achieved a yield strength of up to 20 MPa, an elastic modulus around 600 MPa, and an elongation-at-failure improvement of up to 70% by using a filler loading of up to 3 wt.%. Furthermore, authors successfully evaluated both the proteins' adsorption on the surface of composites and biophysical precursor process of cell adhesion by using serum albumin. As mentioned before, the presence of a small amount of graphene could dramatically improve the protein interaction on the interphase. Additionally, authors grew osteoblast and human mesenchymal stem cells lines on the composites by showing a significant increase in metabolic cell activity and proliferation.

The other interesting class of biomaterials based on graphene and its related derivatives is represented by metal alloys [141]. Graphene promoted the strengthening mechanism of metal alloys due to its excellent bonding interfaces compared with that of traditional alloys [142]. There are still many challenges on the board such as the dispersion of graphene and its related materials into a metal matrix, which is generally done through chemical [143] or mechanical mixing [144] and electrode deposition methods [145]. All of these composites have found interesting biological applications [146].

Escudero et al. [147] electrochemically used rGO for the production of a cobalt /chromium alloy revealing an sp^2 bonding together with the presence of oxygenated groups at the interphase between rGO and the metal matrix. The authors tested the biocompatibility of this material by using mouse macrophage J774A.1 cell line, monitoring the ratio between lactate dehydrogenase and mitochondrial activities. Compared with the neat CoCr alloy, the rGO-based composite promoted the presence of well-distributed and well-shaped macrophages. Additionally, vimentin expression was unaltered, proving the enhanced biocompatibility. In vivo tests were run by survivor ability intraperitoneal injection in Wistar rats. The primary interaction with red blood cells showed a reduction of their size raising some concerns about the in vivo properties.

Nonetheless, coatings produced by using GO have been used by Gao et al. [148] to reduce the corrosion rate of magnesium alloy. Magnesium alloys are ideal materials for cardiovascular stents, but they are prone to corrosion [149]. The authors proved that a chitosan/heparinized GO multilayer coating enhanced the corrosion resistance by reducing the haemolysis rate and platelet adhesion and promoting the adhesion and proliferation of endothelial cells.

Golzar et al. [150] used a similar approach by producing GO/magnesium nanohybrids for enhancing the osteoinductive capability of 3D-printed calcium phosphate-based scaffolds. This material aimed to be highly compatible with dental pulp stem cells. Authors firstly modified rGO by combining it with gelatine and mixed it with phosphates. Then, an enhancement of mechanical features, cell proliferation, and differentiation is achieved. Furthermore, they observed an up-regulation of bone-related genes and proteins COL-I, RUNX2, OCN.

Shahin et al. [151] confirmed the suitability of graphene and magnesium for the production of orthopaedic hard-tissue replacement applications. By only a 0.1 wt.% of graphene nanoplates mixed with magnesium and zirconium, authors observed an improvement of wear resistance by 92% at 200 μN and a reduction of both wear depth and coefficient of friction of the alloy.

Lascano et al. [152] reported a step forward in the use of graphene and its related composites for tissue engineering applications. The authors produced a spongy Nb–Ta–xMn alloy (x: 2, 4, and 6 wt.%) coated with graphene/Ti alloy, reducing the cytotoxicity and improving the biocompatibility upon that of uncoated material. Moreover, in this case, graphene coating improved the cell adhesion and proliferation without compromising the cell morphology.

Su et al. [153] went in deep in the topic by studying the osteoimmunomodulatory role to enhance osteogenesis of titanium coated with GO. The authors evaluated the ability to stimulate the expression of osteogenic genes and extracellular matrix mineralization in human mesenchymal stromal cells. They found that GO-coated surfaces could induce the polarization of macrophages and expression of inflammatory cytokines via the Toll-like receptor pathway. In vivo, GO-coated titanium activated macrophages and induced mild inflammation and a pro-osteogenic environment, with a slight increase in the levels of proinflammatory cytokines. In the meanwhile, an improved expression of TGF-β1 and oncostatin M genes is verified.

Li et al. [154] proposed an interesting application for sintered rGO flakes and liquid rGO/titania material as a synthetic keratoprosthesis skirt for end-stage corneal disorders. These authors observed an improvement of mechanical and chemical properties together with a better wear and corrosion resistance for a loading of 1 wt.%. In vivo studies were carried out by implanting to rabbit corneas without observing any immune and inflammatory responses.

Regenerative medicine is another field where graphene-based materials have released their full potential [155,156]. The adherence of a cell on graphene is a critical property as shown by Morçimen et al. [157]. By studying the adherence and proliferation of the SH-SY5Y neuron cell line on graphene foams, authors proved the viability of this approach in more complex procedures.

Feng et al. [158] produced an iron-oxide-based, magnetic, electrospun, short nanofibre-wrapped GO for a guiding cellular behaviour as shown in Figure 4.
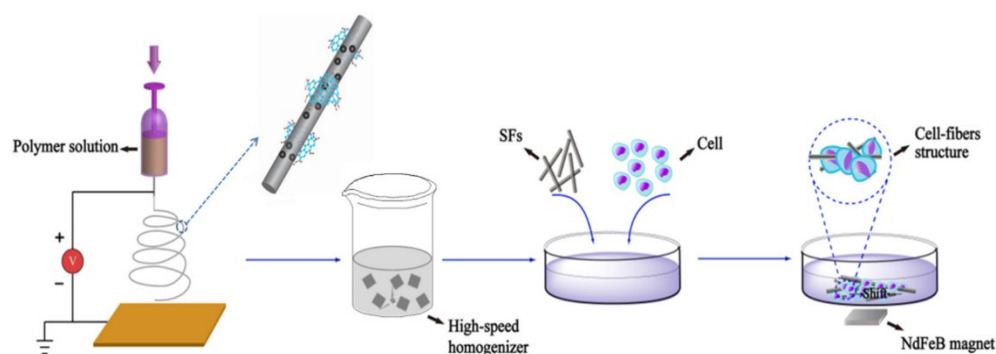
Figure 4. Cellular guidance induced by magnetic GO fibres as described by Feng et al. [158].

As shown in Figure 4, the authors produced short GO magnetic fibres by electrospinning techniques achieving materials with diameters of up to 300 nm and a length of up to 80 µm and a magnetization saturation of up to 50.33 emu/g. These fibres were able to induce an extremely tight adhesion with cells due to the functionalized GO. The observations were particularly promising for tissues manipulation by using external magnetic fields to selectively move specific cellular groups by tailoring the GO surface. Furthermore, the creation of controlled cellular aggregates could be a step forward in specific site repairing.

Agarwal et al. [159] produced a highly elastic and electroconductive graphene /collagen cryogel for spinal cord regeneration. Firstly, the authors tailored the graphene surface with amine residues promoting an efficient cross-linking with collagen showing a conductivity of up to 3.8 ± 0.2 mS/cm and a Young modulus of up to 347 kPa. The authors tested this composite for stem cell transplantation and neural tissue regeneration through the cryogelation approach by using the BM-MSCs cell line. They reported a good stem cell growth and expression enhancement of *CD90* and *CD73* gene upon electric stimulation of up to 100 mV/mm without the loss of stemness. Additionally, the authors observed an ATP secretion increment that could be helpful to favour neuronal regeneration and immunomodulation. Graphene-based cryogel promoted the neuronal differentiation of BM-MSCs with enhanced expression of MAP-2 kinase and β-tubulin III. In vitro observation proved a high indoleamine 2,3 dioxygenase activity under inflammatory conditions together with the proliferation of macrophages, which could aid in tissue repair.

Cellular proliferation is the other relevant task to be faced. Sekuła-Stryjewska et al. [160] studied both GO and rGO as promoting agents for the cardiomyogenic and angiogenic differentiation capacity of human mesenchymal stem cells in vitro. The authors showed that, generally, those substrates fit the requirements for cellular proliferation with the exception of small GO flakes and highly reduced rGO, which decreased proliferation by inducing apoptosis. Nonetheless, this study proved that both GO and rGO did not alter stem cells' phenotype and cell cycle progression while they could tune their adhesive capabilities of these cells. These properties could be used in ocular regenerative medicine as reported by Zambrano-Andazol et al. [161] as a sound replacement for functionalized hydrogels [162].

Ginestra et al. [163] realized poly(caprolactone) mixed with graphene for nerve tissue engineering through electrospinning. Nanofibrous composites showed good properties for the proliferation of rat stem cells with a preferential differentiation to dopaminergic neuronal cells with the increment of graphene percentage.

Similarly, Polo et al. [164] produced nanostructured scaffolds based on copolymers (poly(lactic acid)-poly(caprolactone)) containing GO, aiming to induce the aligned migration and accelerate the neuronal differentiation of neural stem cells. Authors proved the ability to re-establish the spatially oriented neural precursor cell connectivity of this material.

Park et al. [165] used the highly conductive properties of graphene-based hydrogel for the realization of artificial muscles. The hydrogel was produced by incorporating GO into poly(acrylamide) using femtosecond laser ablation and a chemical reduction.

In vitro studies with C2C12 myoblasts revealed that the micropatterned graphene hydrogel induced the myogenesis and myotube alignment. In vivo implantation studies showed a good tissue compatibility.

Techaniyom et al. [166] showed that osteoblast differentiation and gene expression could also be modulated by GO coating of titanium materials due to an upregulation of the expression of the bone matrix protein genes during late-stage osteoblast differentiation.

3.4. From Material to Supramolecular Cluster: Graphene Quantum Dots

Graphene and its related derivatives lack of some properties such as bandgap or optical properties. This reduces the possible applications, and an engineered material could offset these limitations. In recent times, graphene quantum dots (GQDs) have received great attention for their possible unique applications [167] as a solid alternative to classical graphene, GO, and rGO.

Graphene quantum dots consist of graphene sheets, which could be single-sheet or multi-layered. They are nanoparticles with dimensions smaller than 100 nm, commonly under 20 nm, and their shapes are usually circular or elliptical. However, other shapes are produced with different synthetic routes [168].

The synthesis methods to produce GQDs are both top–down and bottom–up as summarized in Figure 5 by using different precursors and synthetic strategies.
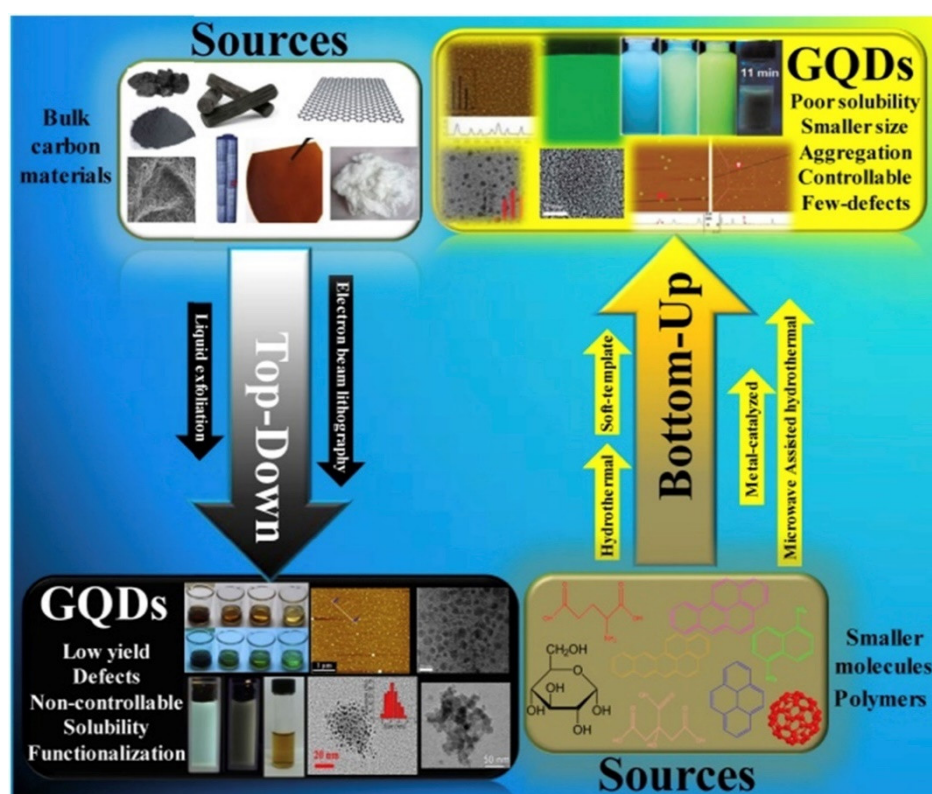

Figure 5. Scheme of graphene quantum dots (GQDs) top–down and bottom–up approaches as reported by [169] (under CC license).

The most common approach is the top–down one that usually consists of physical processes that reduce the dimensions of carbon materials as carbon fibres [170] or coal [171], along with acid oxidation [172] and hydrothermal treatment [173]. Solvothermal route [174], microwave [175], and sonication [176] are also promising alternative approaches.

A top–down physical process is the acid exfoliation, followed by the oxidation of the nano-obtained product. Li et al. [177] suggested an electrochemical synthesis route to produce a variety of GQDs, although the products differ in size, emission colours, and

other intrinsic properties. Hydrothermal synthesis can be done just on precise precursors, such as GO, with a functionalization with oxidizing agents to introduce functional groups on the product surface [178].

The bottom–up method provides for the generation of aromatic molecules as precursors and can lead to high yield. Li et al. [179] developed a protocol to fabricate GQDs through direct pyrolysis on citric acid.

The synthesis routes mentioned above lead to a differentiation of the GQDs produced and their different physicochemical properties which depend on procedure, precursors, defects, and functional groups [180,181]. The GQDs' properties of interest are absorbance, photoluminescence (PL), electrochemical photoluminescence among the optical ones and of course their biocompatibility; all these properties make them great candidates for bioimaging and theragnostic applications.

The absorption characteristics of GQDs are shown in the short-wavelength region because of C=C bonds and around 270–390 nm they show peaks for the C=O bonds. The passivation of the surface with a functional group can alter the disposition of the peaks; it strongly depends on the type of dot.

The principal and most fascinating property of the carbon dots is their photoluminescence. The unclear photoluminescence mechanism is one of the impediments to understand completely the physical mechanism behind these promising materials. The tuneable property of photoluminescence is size-dependent since it is related to quantum confinement. Moreover, other factors such as shape, defect, and doping also influence the effect. In detail, Zhu et al. [182] reported that PL is related to the quantum confinement effect of the electrons in sp^2 carbons [183]. Another structure-dependent characteristic of GQDs is the electron transfer [184]. Biocompatibility and almost absent toxicity make them eligible for in vivo applications. In vitro studies have been made by Shang et al. [185], and they studied the GQDs' effects on the cellular life finding out how the nanomaterial did not affect either the viability or the reproduction capacity. In vivo studies have been made on mice by exposing them to different nanomaterials. The results showed no abnormalities in organs or habits and brought to awareness their excellent biocompatibility, raising interest in the possible bio-applications.

The possible bio-applications of GQDs are cellular imaging [186], real-time in vivo biosensing [187], and drug delivery [188].

The main advantages of GQDs upon traditional imaging solution is related to the extremely high biocompatibility together with facile tailoring properties. Furthermore, the metabolic excretion after the procedure promotes a rapid removal of toxic formulation elements, e.g., heavy metals such as gadolinium or europium used in imaging procedures [189].

4. Conclusions

As we reported, graphene and its related materials have become top players in the crucial production of advanced materials for biological applications.

The features of graphene and its related materials represent a cutting-edge tool for the synthesis of new highly compatible biomaterials that can lead the way for a game changing approach for both drug delivery and regenerative medicine.

Balancing performances and cytotoxicity together with production routes remains the heart of all decision process, and graphene materials are gaining even more space in the field of frontier medicine.

We firmly believe that the high tunability and the good electrical properties represent a starting benchmark to spread the use of graphene across biological applications. These factors would increase its competitiveness, leading graphene materials to a bright future.

References

1. Emerich, D.F.; Thanos, C.G. Nanotechnology and medicine. *Expert Opin. Biol. Ther.* **2003**, *3*, 655–663. [CrossRef] [PubMed]
2. Lu, S.-N.; Xie, N.; Feng, L.-C.; Zhong, J. Applications of nanostructured carbon materials in constructions: The state of the art. *J. Nanomater.* **2015**, *2015*, 1–10. [CrossRef]
3. Candelaria, S.L.; Shao, Y.; Zhou, W.; Li, X.; Xiao, J.; Zhang, J.-G.; Wang, Y.; Liu, J.; Li, J.; Cao, G. Nanostructured carbon for energy storage and conversion. *Nano Energy* **2012**, *1*, 195–220. [CrossRef]
4. Xu, Y.J.; Weinberg, G.; Liu, X.; Timpe, O.; Schlögl, R.; Su, D.S. Nanoarchitecturing of activated carbon: Facile strategy for chemical functionalization of the surface of activated carbon. *Adv. Funct. Mater.* **2008**, *18*, 3613–3619. [CrossRef]
5. Wei, D.; Kivioja, J. Graphene for energy solutions and its industrialization. *Nanoscale* **2013**, *5*, 10108–10126. [CrossRef] [PubMed]
6. Graphene Flagship. Available online: https://graphene-flagship.eu/ (accessed on 17 December 2020).
7. Yang, G.; Li, L.; Lee, W.B.; Ng, M.C. Structure of graphene and its disorders: A review. *Sci. Technol. Adv. Mater.* **2018**, *19*, 613–648. [CrossRef]
8. Ji, X.; Xu, Y.; Zhang, W.; Cui, L.; Liu, J. Review of functionalization, structure and properties of graphene/polymer composite fibers. *Compos. Part A Appl. Sci. Manuf.* **2016**, *87*, 29–45. [CrossRef]
9. Giorcelli, M.; Bartoli, M. Carbon Nanostructures for Actuators: An Overview of Recent Developments. *Actuators* **2019**, *8*, 46. [CrossRef]
10. Lavagna, L.; Massella, D.; Priola, E.; Pavese, M. Relationship between oxygen content of graphene and mechanical properties of cement-based composites. *Cem. Concr. Compos.* **2021**, *115*, 103851. [CrossRef]
11. Lavagna, L.; Marchisio, S.; Merlo, A.; Nisticò, R.; Pavese, M. Polyvinyl butyral-based composites with carbon nanotubes: Efficient dispersion as a key to high mechanical properties. *Polym. Compos.* **2020**. [CrossRef]
12. Kumar, A.; Sharma, K.; Dixit, A.R. A review of the mechanical and thermal properties of graphene and its hybrid polymer nanocomposites for structural applications. *J. Mater. Sci.* **2019**, *54*, 5992–6026. [CrossRef]
13. Dadkhah, M.; Saboori, A.; Fino, P. An overview of the recent developments in metal matrix nanocomposites reinforced by graphene. *Materials* **2019**, *12*, 2823. [CrossRef] [PubMed]
14. Hidalgo-Manrique, P.; Lei, X.; Xu, R.; Zhou, M.; Kinloch, I.A.; Young, R.J. Copper/graphene composites: A review. *J. Mater. Sci.* **2019**, *54*, 12236–12289. [CrossRef]
15. Bartoli, M.; Giorcelli, M.; Jagdale, P.; Rovere, M.; Tagliaferro, A. A Review of Non-Soil Biochar Applications. *Materials* **2020**, *13*, 261. [CrossRef] [PubMed]
16. Strongone, V.; Bartoli, M.; Jagdale, P.; Arrigo, R.; Tagliaferro, A.; Malucelli, G. Preparation and Characterization of UV-LED Curable Acrylic Films Containing Biochar and/or Multiwalled Carbon Nanotubes: Effect of the Filler Loading on the Rheological, Thermal and Optical Properties. *Polymers* **2020**, *12*, 796. [CrossRef]
17. Savi, P.; Yasir, M.; Bartoli, M.; Giorcelli, M.; Longo, M. Electrical and Microwave Characterization of Thermal Annealed Sewage Sludge Derived Biochar Composites. *Appl. Sci.* **2020**, *10*, 1334. [CrossRef]
18. Noori, A.; Bartoli, M.; Frache, A.; Piatti, E.; Giorcelli, M.; Tagliaferro, A. Development of Pressure-Responsive PolyPropylene and Biochar-Based Materials. *Micromachines* **2020**, *11*, 339. [CrossRef]
19. Barbalini, M.; Bartoli, M.; Tagliaferro, A.; Malucelli, G. Phytic Acid and Biochar: An Effective All Bio-Sourced Flame Retardant Formulation for Cotton Fabrics. *Polymers* **2020**, *12*, 811. [CrossRef]
20. Arrigo, R.; Bartoli, M.; Malucelli, G. Poly (lactic Acid)–Biochar Biocomposites: Effect of Processing and Filler Content on Rheological, Thermal, and Mechanical Properties. *Polymers* **2020**, *12*, 892. [CrossRef]
21. Giorcelli, M.; Bartoli, M. Development of Coffee Biochar Filler for the Production of Electrical Conductive Reinforced Plastic. *Polymers* **2019**, *11*, 1916. [CrossRef]
22. Bartoli, M.; Giorcelli, M.; Rosso, C.; Rovere, M.; Jagdale, P.; Tagliaferro, A. Influence of Commercial Biochar Fillers on Brittle-ness/Ductility of Epoxy Resin Composites. *Appl. Sci.* **2019**, *9*, 3109. [CrossRef]
23. Arrigo, R.; Jagdale, P.; Bartoli, M.; Tagliaferro, A.; Malucelli, G. Structure–Property Relationships in Polyethylene-Based Composites Filled with Biochar Derived from Waste Coffee Grounds. *Polymers* **2019**, *11*, 1336. [CrossRef] [PubMed]
24. Priyadarsini, S.; Mohanty, S.; Mukherjee, S.; Basu, S.; Mishra, M. Graphene and graphene oxide as nanomaterials for medicine and biology application. *J. Nanostruct. Chem.* **2018**, *8*, 123–137. [CrossRef]
25. Leachman, S.A.; Merlino, G. Medicine: The final frontier in cancer diagnosis. *Nature* **2017**, *542*, 36–38. [CrossRef]
26. Wender, P.A.; Miller, B.L. Synthesis at the molecular frontier. *Nature* **2009**, *460*, 197–201. [CrossRef]
27. Bartoli, M.; Jagdale, P.; Tagliaferro, A. A Short Review on Biomedical Applications of Nanostructured Bismuth Oxide and Related Nanomaterials. *Materials* **2020**, *13*, 5234. [CrossRef]
28. Ivorra, M.; Paya, M.; Villar, A. A review of natural products and plants as potential antidiabetic drugs. *J. Ethnopharmacol.* **1989**, *27*, 243–275. [CrossRef]

29. Rosen, H.; Abribat, T. The rise and rise of drug delivery. *Nat. Rev. Drug Discov.* **2005**, *4*, 381–385. [CrossRef]

30. DeWitt, N. Regenerative medicine. *Nature* **2008**, *453*, 301. [CrossRef]

31. Zarrintaj, P.; Mostafapoor, F.; Milan, P.B.; Saeb, M.R. Theranostic platforms proposed for cancerous stem cells: A review. *Curr. Stem Cell Res. Ther.* **2019**, *14*, 137–145. [CrossRef]

32. Place, E.S.; Evans, N.D.; Stevens, M.M. Complexity in biomaterials for tissue engineering. *Nat. Mater.* **2009**, *8*, 457–470. [CrossRef] [PubMed]

33. Aminov, R.I. The role of antibiotics and antibiotic resistance in nature. *Environ. Microbiol.* **2009**, *11*, 2970–2988. [CrossRef] [PubMed]

34. Mintmire, J.W.; Dunlap, B.I.; White, C.T. Are fullerene tubules metallic? *Phys. Rev. Lett.* **1992**, *68*, 631. [CrossRef] [PubMed]

35. Yan, J.-A.; Ruan, W.; Chou, M. Electron-phonon interactions for optical-phonon modes in few-layer graphene: First-principles calculations. *Phys. Rev. B* **2009**, *79*, 115443. [CrossRef]

36. Dresselhaus, M.; Jorio, A.; Saito, R. Characterizing graphene, graphite, and carbon nanotubes by Raman spectroscopy. *Annu. Rev. Condens. Matter Phys.* **2010**, *1*, 89–108. [CrossRef]

37. Rhee, K.Y. Electronic and Thermal Properties of Graphene. *Nanomaterials* **2020**, *10*, 926. [CrossRef] [PubMed]

38. Lee, H.C.; Liu, W.-W.; Chai, S.-P.; Mohamed, A.R.; Lai, C.W.; Khe, C.-S.; Voon, C.; Hashim, U.; Hidayah, N. Synthesis of single-layer graphene: A review of recent development. *Procedia Chem.* **2016**, *19*, 916–921. [CrossRef]

39. Narita, A.; Wang, X.-Y.; Feng, X.; Müllen, K. New advances in nanographene chemistry. *Chem. Soc. Rev.* **2015**, *44*, 6616–6643. [CrossRef]

40. Sun, Z.; Fang, S.; Hu, Y.H. 3D Graphene Materials: From Understanding to Design and Synthesis Control. *Chem. Rev.* **2020**. [CrossRef]

41. Brisebois, P.; Siaj, M. Harvesting graphene oxide–years 1859 to 2019: A review of its structure, synthesis, properties and exfoliation. *J. Mater. Chem. C* **2020**, *8*, 1517–1547. [CrossRef]

42. Brodie, B.C. XIII. On the atomic weight of graphite. *Philos. Trans. R. Soc. Lond.* **1859**, *149*, 249–259.

43. Staudenmaier, L. Verfahren zur darstellung der graphitsäure. *Ber. Dtsch. Chem. Ges.* **1898**, *31*, 1481–1487. [CrossRef]

44. William, S.; Hummers, J.; Offeman, R.E. Preparation of graphitic oxide. *J. Am. Chem. Soc.* **1958**, *80*, 1339.

45. Poh, H.L.; Šaněk, F.; Ambrosi, A.; Zhao, G.; Sofer, Z.; Pumera, M. Graphenes prepared by Staudenmaier, Hofmann and Hummers methods with consequent thermal exfoliation exhibit very different electrochemical properties. *Nanoscale* **2012**, *4*, 3515–3522. [CrossRef] [PubMed]

46. Araújo, M.P.; Soares, O.; Fernandes, A.; Pereira, M.; Freire, C. Tuning the surface chemistry of graphene flakes: New strategies for selective oxidation. *RSC Adv.* **2017**, *7*, 14290–14301. [CrossRef]

47. Szabó, T.; Berkesi, O.; Forgó, P.; Josepovits, K.; Sanakis, Y.; Petridis, D.; Dékány, I. Evolution of surface functional groups in a series of progressively oxidized graphite oxides. *Chem. Mater.* **2006**, *18*, 2740–2749. [CrossRef]

48. Lavagna, L.; Meligrana, G.; Gerbaldi, C.; Tagliaferro, A.; Bartoli, M. Graphene and Lithium-Based Battery Electrodes: A Review of Recent Literature. *Energies* **2020**, *13*, 4867. [CrossRef]

49. Lerf, A.; He, H.; Riedl, T.; Forster, M.; Klinowski, J. 13C and 1H MAS NMR studies of graphite oxide and its chemically modified derivatives. *Solid State Ion.* **1997**, *101*, 857–862. [CrossRef]

50. Thakur, S.; Karak, N. Alternative methods and nature-based reagents for the reduction of graphene oxide: A review. *Carbon* **2015**, *94*, 224–242. [CrossRef]

51. Guex, L.G.; Sacchi, B.; Peuvot, K.F.; Andersson, R.L.; Pourrahimi, A.M.; Ström, V.; Farris, S.; Olsson, R.T. Experimental review: Chemical reduction of graphene oxide (GO) to reduced graphene oxide (rGO) by aqueous chemistry. *Nanoscale* **2017**, *9*, 9562–9571. [CrossRef]

52. Liu, S.; Tian, J.; Wang, L.; Sun, X. A method for the production of reduced graphene oxide using benzylamine as a reducing and stabilizing agent and its subsequent decoration with Ag nanoparticles for enzymeless hydrogen peroxide detection. *Carbon* **2011**, *49*, 3158–3164. [CrossRef]

53. Lee, X.J.; Hiew, B.Y.Z.; Lai, K.C.; Lee, L.Y.; Gan, S.; Thangalazhy-Gopakumar, S.; Rigby, S. Review on graphene and its derivatives: Synthesis methods and potential industrial implementation. *J. Taiwan Inst. Chem. Eng.* **2019**, *98*, 163–180. [CrossRef]

54. Muñoz, R.; Gómez-Aleixandre, C. Review of CVD synthesis of graphene. *Chem. Vap. Depos.* **2013**, *19*, 297–322. [CrossRef]

55. Khurana, G.; Misra, P.; Katiyar, R.S. Multilevel resistive memory switching in graphene sandwiched organic polymer heterostructure. *Carbon* **2014**, *76*, 341–347. [CrossRef]

56. Li, W.; Li, D.; Fu, Q.; Pan, C. Conductive enhancement of copper/graphene composites based on high-quality graphene. *RSC Adv.* **2015**, *5*, 80428–80433. [CrossRef]

57. Choi, H.; Kim, H.; Hwang, S.; Choi, W.; Jeon, M. Dye-sensitized solar cells using graphene-based carbon nano composite as counter electrode. *Sol. Energy Mater. Sol. Cells* **2011**, *95*, 323–325. [CrossRef]

58. Gao, Y.; Jing, H.W.; Chen, S.J.; Du, M.R.; Chen, W.Q.; Duan, W.H. Influence of ultrasonication on the dispersion and enhancing effect of graphene oxide–carbon nanotube hybrid nanoreinforcement in cementitious composite. *Compos. Part B Eng.* **2019**, *164*, 45–53. [CrossRef]

59. Liu, Y.; Zhang, B.; Xu, Q.; Hou, Y.; Seyedin, S.; Qin, S.; Wallace, G.G.; Beirne, S.; Razal, J.M.; Chen, J. Development of graphene oxide/polyaniline inks for high performance flexible microsupercapacitors via extrusion printing. *Adv. Funct. Mater.* **2018**, *28*, 1706592. [CrossRef]

60. Kumar, S.N.; Keshavamurthy, R.; Haseebuddin, M.; Koppad, P.G. Mechanical properties of aluminium-graphene composite synthesized by powder metallurgy and hot extrusion. *Trans. Indian Inst. Met.* **2017**, *70*, 605–613. [CrossRef]

61. Melanitis, N.; Tetlow, P.L.; Galiotis, C. Characterization of PAN-based carbon fibres with laser Raman spectroscopy. *J. Mater. Sci.* **1996**, *31*, 851–860. [CrossRef]

62. Koenig, F. Raman spectrum of graphite. *J. Chem. Phys.* **1970**, *53*, 5.

63. Shukla, S.; Saxena, S. Spectroscopic investigation of confinement effects on optical properties of graphene oxide. *Appl. Phys. Lett.* **2011**, *98*, 073104. [CrossRef]

64. Sun, Z.; Yan, Z.; Yao, J.; Beitler, E.; Zhu, Y.; Tour, J.M. Growth of graphene from solid carbon sources. *Nature* **2010**, *468*, 549–552. [CrossRef] [PubMed]

65. Chen, X.; Wang, X.; Fang, D. A review on C1s XPS-spectra for some kinds of carbon materials. *Fuller. Nanotub. Carbon Nanostruct.* **2020**, *28*, 1048–1058. [CrossRef]

66. Torrengo, S.; Canteri, R.; Dell'Anna, R.; Minati, L.; Pasquarelli, A.; Speranza, G. XPS and ToF-SIMS investigation of nanocrystalline diamond oxidized surfaces. *Appl. Surf. Sci.* **2013**, *276*, 101–111. [CrossRef]

67. Zhang, Y.; Tamijani, A.A.; Taylor, M.E.; Zhi, B.; Haynes, C.L.; Mason, S.E.; Hamers, R.J. Molecular Surface Functionalization of Carbon Materials via Radical-Induced Grafting of Terminal Alkenes. *J. Am. Chem. Soc.* **2019**, *141*, 8277–8288. [CrossRef]

68. Rathnayake, R.M.N.M.; Wijayasinghe, H.W.M.A.C.; Pitawala, H.M.T.G.A.; Yoshimura, M.; Huang, H.-H. Synthesis of graphene oxide and reduced graphene oxide by needle platy natural vein graphite. *Appl. Surf. Sci.* **2017**, *393*, 309–315. [CrossRef]

69. Malinský, P.; Macková, A.; Mikšová, R.; Kováčiková, H.; Cutroneo, M.; Luxa, J.; Bouša, D.; Štrochová, B.; Sofer, Z. Graphene oxide layers modified by light energetic ions. *Phys. Chem. Chem. Phys.* **2017**, *19*, 10282–10291. [CrossRef]

70. Cooper, A.J.; Wilson, N.R.; Kinloch, I.A.; Dryfe, R.A.W. Single stage electrochemical exfoliation method for the production of few-layer graphene via intercalation of tetraalkylammonium cations. *Carbon* **2014**, *66*, 340–350. [CrossRef]

71. Zhang, H.-B.; Zheng, W.-G.; Yan, Q.; Yang, Y.; Wang, J.-W.; Lu, Z.-H.; Ji, G.-Y.; Yu, Z.-Z. Electrically conductive polyethylene terephthalate/graphene nanocomposites prepared by melt compounding. *Polymer* **2010**, *51*, 1191–1196. [CrossRef]

72. Li, D.; Müller, M.B.; Gilje, S.; Kaner, R.B.; Wallace, G.G. Processable aqueous dispersions of graphene nanosheets. *Nat. Nanotechnol.* **2008**, *3*, 101–105. [CrossRef] [PubMed]

73. Lee, C.; Wei, X.; Kysar, J.W.; Hone, J. Measurement of the Elastic Properties and Intrinsic Strength of Monolayer Graphene. *Science* **2008**, *321*, 385–388. [CrossRef] [PubMed]

74. Guo, K.W.; Tam, H.-Y. TEM Morphology of Carbon Nanotubes (CNTs) and its Effect on the Life of Micropunch. *Transm. Electron Microsc. Theory Appl.* **2015**. [CrossRef]

75. Liu, Z.; Suenaga, K.; Harris, P.J.; Iijima, S. Open and closed edges of graphene layers. *Phys. Rev. Lett.* **2009**, *102*, 015501. [CrossRef]

76. Coats, A.; Redfern, J. Thermogravimetric analysis. A review. *Analyst* **1963**, *88*, 906–924. [CrossRef]

77. Lavagna, L.; Musso, S.; Pavese, M. A facile method to oxidize carbon nanotubes in controlled flow of oxygen at 350 °C. *Mater. Lett.* **2021**, *283*, 128816. [CrossRef]

78. Leenaerts, O.; Partoens, B.; Peeters, F. Water on graphene: Hydrophobicity and dipole moment using density functional theory. *Phys. Rev. B* **2009**, *79*, 235440. [CrossRef]

79. Mullick Chowdhury, S.; Lalwani, G.; Zhang, K.; Yang, J.Y.; Neville, K.; Sitharaman, B. Cell specific cytotoxicity and uptake of graphene nanoribbons. *Biomaterials* **2013**, *34*, 283–293. [CrossRef]

80. Mu, Q.; Su, G.; Li, L.; Gilbertson, B.O.; Yu, L.H.; Zhang, Q.; Sun, Y.-P.; Yan, B. Size-Dependent Cell Uptake of Protein-Coated Graphene Oxide Nanosheets. *ACS Appl. Mater. Interfaces* **2012**, *4*, 2259–2266. [CrossRef]

81. Zhang, Q.; Wu, Z.; Li, N.; Pu, Y.; Wang, B.; Zhang, T.; Tao, J. Advanced review of graphene-based nanomaterials in drug delivery systems: Synthesis, modification, toxicity and application. *Mater. Sci. Eng. C* **2017**, *77*, 1363–1375. [CrossRef]

82. Cherian, R.; Ashtami, J.; Mohanan, P. Effect of surface modified reduced graphene oxide nanoparticles on cerebellar granule neurons. *J. Drug Deliv. Sci. Technol.* **2020**, *58*, 101706. [CrossRef]

83. Luo, R.; Zhou, H.; Dang, W.; Long, Y.; Tong, C.; Xie, Q.; Daniyal, M.; Liu, B.; Wang, W. A DNAzyme-rGO coupled fluorescence assay for T4PNK activity in vitro and intracellular imaging. *Sens. Actuators B Chem.* **2020**, *310*, 127884. [CrossRef]

84. Yang, K.; Feng, L.; Liu, Z. Stimuli responsive drug delivery systems based on nano-graphene for cancer therapy. *Adv. Drug Deliv. Rev.* **2016**, *105*, 228–241. [CrossRef] [PubMed]

85. Depan, D.; Shah, J.; Misra, R. Controlled release of drug from folate-decorated and graphene mediated drug delivery system: Synthesis, loading efficiency, and drug release response. *Mater. Sci. Eng. C* **2011**, *31*, 1305–1312. [CrossRef]

86. Murakami, T.; Tsuchida, K. Recent advances in inorganic nanoparticle-based drug delivery systems. *Mini Rev. Med. Chem.* **2008**, *8*, 175.

87. Suggs, K.; Reuven, D.; Wang, X.-Q. Electronic properties of cycloaddition-functionalized graphene. *J. Phys. Chem. C* **2011**, *115*, 3313–3317. [CrossRef]

88. Quintana, M.; Spyrou, K.; Grzelczak, M.; Browne, W.R.; Rudolf, P.; Prato, M. Functionalization of graphene via 1, 3-dipolar cycloaddition. *ACS Nano* **2010**, *4*, 3527–3533. [CrossRef]

89. Strom, T.A.; Dillon, E.P.; Hamilton, C.E.; Barron, A.R. Nitrene addition to exfoliated graphene: A one-step route to highly functionalized graphene. *Chem. Commun.* **2010**, *46*, 4097–4099. [CrossRef]

90. Castillo, A.E.R.; VanáTendeloo, G. Selective organic functionalization of graphene bulk or graphene edges. *Chem. Commun.* **2011**, *47*, 9330–9332.

91. Tiwari, G.; Tiwari, R.; Sriwastawa, B.; Bhati, L.; Pandey, S.; Pandey, P.; Bannerjee, S.K. Drug delivery systems: An updated review. *Int. J. Pharm. Investig.* **2012**, *2*, 2. [CrossRef]

92. Zhang, Y.; Wu, C.; Guo, S.; Zhang, J. Interactions of graphene and graphene oxide with proteins and peptides. *Nanotechnol. Rev.* **2013**, *2*, 27–45. [CrossRef]

93. Wang, Y.; Wang, C. Self-assembly of graphene sheets actuated by surface topological defects: Toward the fabrication of novel nanostructures and drug delivery devices. *Appl. Surf. Sci.* **2020**, *505*, 144008. [CrossRef]

94. Mohammed, M.H.; Hanoon, F.H. Theoretical prediction of delivery and adsorption of various anticancer drugs into pristine and metal-doped graphene nanosheet. *Chin. J. Phys.* **2020**, *68*, 578–595. [CrossRef]

95. Mauri, E.; Salvati, A.; Cataldo, A.; Mozetic, P.; Basoli, F.; Abbruzzese, F.; Trombetta, M.; Bellucci, S.; Rainer, A. Graphene-laden hydrogels: A strategy for thermally triggered drug delivery. *Mater. Sci. Eng. C* **2021**, *118*, 111353. [CrossRef]

96. Ezzati, N.; Mahjoub, A.R.; Shokrollahi, S.; Amiri, A.; Abolhosseini Shahrnoy, A. Novel Biocompatible Amino Acids-Functionalized Three-dimensional Graphene Foams: As the Attractive and Promising Cisplatin Carriers for Sustained Release Goals. *Int. J. Pharm.* **2020**, *589*, 119857. [CrossRef]

97. Abdel-Bary, A.S.; Tolan, D.A.; Nassar, M.Y.; Taketsugu, T.; El-Nahas, A.M. Chitosan, magnetite, silicon dioxide, and graphene oxide nanocomposites: Synthesis, characterization, efficiency as cisplatin drug delivery, and DFT calculations. *Int. J. Biol. Macromol.* **2020**, *154*, 621–633. [CrossRef]

98. Trusek, A.; Kijak, E.; Granicka, L. Graphene oxide as a potential drug carrier—Chemical carrier activation, drug attachment and its enzymatic controlled release. *Mater. Sci. Eng. C* **2020**, *116*, 111240. [CrossRef]

99. Keizer, H.; Pinedo, H.; Schuurhuis, G.; Joenje, H. Doxorubicin (adriamycin): A critical review of free radical-dependent mechanisms of cytotoxicity. *Pharmacol. Ther.* **1990**, *47*, 219–231. [CrossRef]

100. Shen, J.-W.; Li, J.; Dai, J.; Zhou, M.; Ren, H.; Zhang, L.; Hu, Q.; Kong, Z.; Liang, L. Molecular dynamics study on the adsorption and release of doxorubicin by chitosan-decorated graphene. *Carbohydr. Polym.* **2020**, *248*, 116809. [CrossRef]

101. Kanwal, U.; Irfan Bukhari, N.; Ovais, M.; Abass, N.; Hussain, K.; Raza, A. Advances in nano-delivery systems for doxorubicin: An updated insight. *J. Drug Target.* **2018**, *26*, 296–310. [CrossRef]

102. Ayazi, H.; Akhavan, O.; Raoufi, M.; Varshochian, R.; Hosseini Motlagh, N.S.; Atyabi, F. Graphene aerogel nanoparticles for in-situ loading/pH sensitive releasing anticancer drugs. *Colloids Surf. B Biointerfaces* **2020**, *186*, 110712. [CrossRef] [PubMed]

103. Anirudhan, T.S.; Chithra Sekhar, V.; Athira, V.S. Graphene oxide based functionalized chitosan polyelectrolyte nanocomposite for targeted and pH responsive drug delivery. *Int. J. Biol. Macromol.* **2020**, *150*, 468–479. [CrossRef] [PubMed]

104. Omidi, S.; Pirhayati, M.; Kakanejadifard, A. Co-delivery of doxorubicin and curcumin by a pH-sensitive, injectable, and in situ hydrogel composed of chitosan, graphene, and cellulose nanowhisker. *Carbohydr. Polym.* **2020**, *231*, 115745. [CrossRef] [PubMed]

105. Pourjavadi, A.; Asgari, S.; Hosseini, S.H. Graphene oxide functionalized with oxygen-rich polymers as a pH-sensitive carrier for co-delivery of hydrophobic and hydrophilic drugs. *J. Drug Deliv. Sci. Technol.* **2020**, *56*, 101542. [CrossRef]

106. Alipour, N.; Namazi, H. Chelating ZnO-dopamine on the surface of graphene oxide and its application as pH-responsive and antibacterial nanohybrid delivery agent for doxorubicin. *Mater. Sci. Eng. C* **2020**, *108*, 110459. [CrossRef] [PubMed]

107. Sattari, S.; Tehrani, A.D.; Adeli, M.; Soleimani, K.; Rashidipour, M. Fabrication of new generation of co-delivery systems based on graphene-g-cyclodextrin/chitosan nanofiber. *Int. J. Biol. Macromol.* **2020**, *156*, 1126–1134. [CrossRef]

108. Di Zhang, Q.X.; Wang, N.; Yang, Y.; Liu, J.; Yu, G.; Yang, X.; Xu, H.; Wang, H. A complex micellar system co-delivering curcumin with doxorubicin against cardiotoxicity and tumor growth. *Int. J. Nanomed.* **2018**, *13*, 4549. [CrossRef]

109. Jahanshahi, M.; Kowsari, E.; Haddadi-Asl, V.; Khoobi, M.; Bazri, B.; Aryafard, M.; Lee, J.H.; Kadumudi, F.B.; Talebian, S.; Kamaly, N.; et al. An innovative and eco-friendly modality for synthesis of highly fluorinated graphene by an acidic ionic liquid: Making of an efficacious vehicle for anti-cancer drug delivery. *Appl. Surf. Sci.* **2020**, *515*, 146071. [CrossRef]

110. Razaghi, M.; Ramazani, A.; Khoobi, M.; Mortezazadeh, T.; Aksoy, E.A.; Küçükkılınç, T.T. Highly fluorinated graphene oxide nanosheets for anticancer linoleic-curcumin conjugate delivery and T2-Weighted magnetic resonance imaging: In vitro and in vivo studies. *J. Drug Deliv. Sci. Technol.* **2020**, *60*, 101967. [CrossRef]

111. Zaboli, M.; Raissi, H.; Moghaddam, N.R.; Farzad, F. Probing the adsorption and release mechanisms of cytarabine anticancer drug on/from dopamine functionalized graphene oxide as a highly efficient drug delivery system. *J. Mol. Liq.* **2020**, *301*, 112458. [CrossRef]

112. Li, H.; Jia, Y.; Liu, C. Pluronic®® F127 stabilized reduced graphene oxide hydrogel for transdermal delivery of ondansetron: Ex vivo and animal studies. *Colloids Surf. B Biointerfaces* **2020**, *195*, 111259. [CrossRef] [PubMed]

113. Shahabi, M.; Raissi, H. Payload delivery of anticancer drug Tegafur with the assistance of graphene oxide nanosheet during biomembrane penetration: Molecular dynamics simulation survey. *Appl. Surf. Sci.* **2020**, *517*, 146186. [CrossRef]

114. Abdoli, M.; Sadrjavadi, K.; Arkan, E.; Zangeneh, M.M.; Moradi, S.; Zangeneh, A.; Shahlaei, M.; Khaledian, S. Polyvinyl alcohol/Gum tragacanth/graphene oxide composite nanofiber for antibiotic delivery. *J. Drug Deliv. Sci. Technol.* **2020**, *60*, 102044. [CrossRef]

115. Huang, J.; Jacobsen, J.; Larsen, S.W.; Genina, N.; Van de Weert, M.; Müllertz, A.; Nielsen, H.M.; Mu, H. Graphene oxide as a functional excipient in buccal films for delivery of clotrimazole: Effect of molecular interactions on drug release and antifungal activity in vitro. *Int. J. Pharm.* **2020**, *589*, 119811. [CrossRef]

116. Wang, R.; Gan, J.; Li, R.; Duan, J.; Zhou, J.; Lv, M.; Qi, R. Controlled delivery of ketamine from reduced graphene oxide hydrogel for neuropathic pain: In vitro and in vivo studies. *J. Drug Deliv. Sci. Technol.* **2020**, *60*, 101964. [CrossRef]

117. Pooresmaeil, M.; Javanbakht, S.; Behzadi Nia, S.; Namazi, H. Carboxymethyl cellulose/mesoporous magnetic graphene oxide as a safe and sustained ibuprofen delivery bio-system: Synthesis, characterization, and study of drug release kinetic. *Colloids Surf. A Physicochem. Eng. Asp.* **2020**, *594*, 124662. [CrossRef]

118. Wang, X.; Guo, W.; Li, L.; Yu, F.; Li, J.; Liu, L.; Fang, B.; Xia, L. Photothermally triggered biomimetic drug delivery of Teriparatide via reduced graphene oxide loaded chitosan hydrogel for osteoporotic bone regeneration. *Chem. Eng. J.* **2020**, 127413. [CrossRef]

119. Munir, K.S.; Wen, C.; Li, Y. Carbon nanotubes and graphene as nanoreinforcements in metallic biomaterials: A review. *Adv. Biosyst.* **2019**, *3*, 1800212. [CrossRef]

120. Thompson, B.C.; Murray, E.; Wallace, G.G. Graphite oxide to graphene. Biomaterials to bionics. *Adv. Mater.* **2015**, *27*, 7563–7582. [CrossRef]

121. Wang, Q.; Wang, M.; Wang, K.; Sun, Y.; Zhang, H.; Lu, X.; Duan, K. Molecular mechanisms of interactions between BMP-2 and graphene: Effects of functional groups and microscopic morphology. *Appl. Surf. Sci.* **2020**, *525*, 146636. [CrossRef]

122. Horch, R.E. Future perspectives in tissue engineering:'Tissue Engineering'review series. *J. Cell. Mol. Med.* **2006**, *10*, 4–6. [CrossRef] [PubMed]

123. Shin, S.R.; Li, Y.-C.; Jang, H.L.; Khoshakhlagh, P.; Akbari, M.; Nasajpour, A.; Zhang, Y.S.; Tamayol, A.; Khademhosseini, A. Graphene-based materials for tissue engineering. *Adv. Drug Deliv. Rev.* **2016**, *105*, 255–274. [CrossRef] [PubMed]

124. Bahrami, S.; Solouk, A.; Mirzadeh, H.; Seifalian, A.M. Electroconductive polyurethane/graphene nanocomposite for biomedical applications. *Compos. Part B Eng.* **2019**, *168*, 421–431. [CrossRef]

125. Pant, H.R.; Pokharel, P.; Joshi, M.K.; Adhikari, S.; Kim, H.J.; Park, C.H.; Kim, C.S. Processing and characterization of electrospun graphene oxide/polyurethane composite nanofibers for stent coating. *Chem. Eng. J.* **2015**, *270*, 336–342. [CrossRef]

126. O'Brien, B.; Carroll, W. The evolution of cardiovascular stent materials and surfaces in response to clinical drivers: A review. *Acta Biomater.* **2009**, *5*, 945–958. [CrossRef]

127. Pathmanapan, S.; Periyathambi, P.; Anandasadagopan, S.K. Fibrin hydrogel incorporated with graphene oxide functionalized nanocomposite scaffolds for bone repair—In vitro and in vivo study. *Nanomed. Nanotechnol. Biol. Med.* **2020**, *29*, 102251. [CrossRef] [PubMed]

128. Uhthoff, H.K.; Finnegan, M. The effects of metal plates on post-traumatic remodelling and bone mass. *J. Bone Jt. Surg. Br. Vol.* **1983**, *65*, 66–71. [CrossRef] [PubMed]

129. Sansone, V.; Pagani, D.; Melato, M. The effects on bone cells of metal ions released from orthopaedic implants. A review. *Clin. Cases Miner. Bone Metab.* **2013**, *10*, 34. [CrossRef]

130. Khalili, R.; Zarrintaj, P.; Jafari, S.H.; Vahabi, H.; Saeb, M.R. Electroactive poly (p-phenylene sulfide)/r-graphene oxide/chitosan as a novel potential candidate for tissue engineering. *Int. J. Biol. Macromol.* **2020**, *154*, 18–24. [CrossRef]

131. Xue, J.; Wang, X.; Wang, E.; Li, T.; Chang, J.; Wu, C. Bioinspired multifunctional biomaterials with hierarchical microstructure for wound dressing. *Acta Biomater.* **2019**, *100*, 270–279. [CrossRef]

132. Wang, F.; Jyothirmayee Aravind, S.S.; Wu, H.; Forys, J.; Venkataraman, V.; Ramanujachary, K.; Hu, X. Tunable green graphene-silk biomaterials: Mechanism of protein-based nanocomposites. *Mater. Sci. Eng. C* **2017**, *79*, 728–739. [CrossRef] [PubMed]

133. Daneshmandi, L.; Barajaa, M.; Tahmasbi Rad, A.; Sydlik, S.A.; Laurencin, C.T. Graphene-Based Biomaterials for Bone Regenerative Engineering: A Comprehensive Review of the Field and Considerations Regarding Biocompatibility and Biodegradation. *Adv. Healthc. Mater.* **2020**, 2001414. [CrossRef] [PubMed]

134. Marques, P.A.; Gonçalves, G.; Singh, M.K.; Grácio, J. Graphene oxide and hydroxyapatite as fillers of polylactic acid nanocomposites: Preparation and characterization. *J. Nanosci. Nanotechnol.* **2012**, *12*, 6686–6692. [CrossRef] [PubMed]

135. Chuan, D.; Fan, R.; Wang, Y.; Ren, Y.; Wang, C.; Du, Y.; Zhou, L.; Yu, J.; Gu, Y.; Chen, H. Stereocomplex poly (lactic acid)-based composite nanofiber membranes with highly dispersed hydroxyapatite for potential bone tissue engineering. *Compos. Sci. Technol.* **2020**, *92*, 108107. [CrossRef]

136. Becker, J.M.; Pounder, R.J.; Dove, A.P. Synthesis of poly (lactide) s with modified thermal and mechanical properties. *Macromol. Rapid Commun.* **2010**, *31*, 1923–1937. [CrossRef] [PubMed]

137. Fujishiro, S.; Kan, K.; Akashi, M.; Ajiro, H. Stability of adhesive interfaces by stereocomplex formation of polylactides and hybridization with nanoparticles. *Polym. Degrad. Stab.* **2017**, *141*, 69–76. [CrossRef]

138. Chiesa, E.; Dorati, R.; Pisani, S.; Bruni, G.; Rizzi, L.G.; Conti, B.; Modena, T.; Genta, I. Graphene nanoplatelets for the development of reinforced PLA–PCL electrospun fibers as the next-generation of biomedical mats. *Polymers* **2020**, *12*, 1390. [CrossRef]

139. Lahiri, D.; Dua, R.; Zhang, C.; De Socarraz-Novoa, I.; Bhat, A.; Ramaswamy, S.; Agarwal, A. Graphene Nanoplatelet-Induced Strengthening of UltraHigh Molecular Weight Polyethylene and Biocompatibility In vitro. *ACS Appl. Mater. Interfaces* **2012**, *4*, 2234–2241. [CrossRef]

140. Upadhyay, R.; Naskar, S.; Bhaskar, N.; Bose, S.; Basu, B. Modulation of Protein Adsorption and Cell Proliferation on Polyethylene Immobilized Graphene Oxide Reinforced HDPE Bionanocomposites. *ACS Appl. Mater. Interfaces* **2016**, *8*, 11954–11968. [CrossRef]

141. Hu, Z.; Tong, G.; Lin, D.; Chen, C.; Guo, H.; Xu, J.; Zhou, L. Graphene-reinforced metal matrix nanocomposites–a review. *Mater. Sci. Technol.* **2016**, *32*, 930–953. [CrossRef]

142. Li, J.; Qin, L.; Yang, K.; Ma, Z.; Wang, Y.; Cheng, L.; Zhao, D. Materials evolution of bone plates for internal fixation of bone fractures: A review. *J. Mater. Sci. Technol.* **2020**, *36*, 190–208. [CrossRef]

143. Zeng, X.; Teng, J.; Yu, J.-G.; Tan, A.-S.; Fu, D.-F.; Zhang, H. Fabrication of homogeneously dispersed graphene/Al composites by solution mixing and powder metallurgy. *Int. J. Miner. Metall. Mater.* **2018**, *25*, 102–109. [CrossRef]

144. Khobragade, N.; Sikdar, K.; Kumar, B.; Bera, S.; Roy, D. Mechanical and electrical properties of copper-graphene nanocomposite fabricated by high pressure torsion. *J. Alloys Compd.* **2019**, *776*, 123–132. [CrossRef]

145. García-Argumánez, A.; Llorente, I.; Caballero-Calero, O.; González, Z.; Menéndez, R.; Escudero, M.; García-Alonso, M. Electrochemical reduction of graphene oxide on biomedical grade CoCr alloy. *Appl. Surf. Sci.* **2019**, *465*, 1028–1036. [CrossRef]

146. Kumar, H.P.; Xavior, M.A. Graphene reinforced metal matrix composite (GRMMC): A review. *Procedia Eng.* **2014**, *97*, 1033–1040. [CrossRef]

147. Escudero, M.L.; Llorente, I.; Pérez-Maceda, B.T.; José-Pinilla, S.S.; Sánchez-López, L.; Lozano, R.M.; Aguado-Henche, S.; De Arriba, C.C.; Alobera-Gracia, M.A.; García-Alonso, M.C. Electrochemically reduced graphene oxide on CoCr biomedical alloy: Characterization, macrophage biocompatibility and hemocompatibility in rats with graphene and graphene oxide. *Mater. Sci. Eng. C* **2020**, *109*, 110522. [CrossRef]

148. Gao, F.; Hu, Y.; Gong, Z.; Liu, T.; Gong, T.; Liu, S.; Zhang, C.; Quan, L.; Kaveendran, B.; Pan, C. Fabrication of chitosan/heparinized graphene oxide multilayer coating to improve corrosion resistance and biocompatibility of magnesium alloys. *Mater. Sci. Eng. C* **2019**, *104*, 109947. [CrossRef]

149. Heublein, B.; Rohde, R.; Kaese, V.; Niemeyer, M.; Hartung, W.; Haverich, A. Biocorrosion of magnesium alloys: A new principle in cardiovascular implant technology? *Heart* **2003**, *89*, 651–656. [CrossRef]

150. Golzar, H.; Mohammadrezaei, D.; Yadegari, A.; Rasoulianboroujeni, M.; Hashemi, M.; Omidi, M.; Yazdian, F.; Shalbaf, M.; Tayebi, L. Incorporation of functionalized reduced graphene oxide/magnesium nanohybrid to enhance the osteoinductivity capability of 3D printed calcium phosphate-based scaffolds. *Compos. Part B Eng.* **2020**, *185*, 107749. [CrossRef]

151. Shahin, M.; Munir, K.; Wen, C.; Li, Y. Nano-tribological behavior of graphene nanoplatelet–reinforced magnesium matrix nanocomposites. *J. Magnes. Alloy.* **2020**. [CrossRef]

152. Lascano, S.; Chávez-Vásconez, R.; Muñoz-Rojas, D.; Aristizabal, J.; Arce, B.; Parra, C.; Acevedo, C.; Orellana, N.; Reyes-Valenzuela, M.; Gotor, F.J.; et al. Graphene-coated Ti-Nb-Ta-Mn foams: A promising approach towards a suitable biomaterial for bone replacement. *Surf. Coat. Technol.* **2020**, *401*, 126250. [CrossRef]

153. Su, J.; Du, Z.; Xiao, L.; Wei, F.; Yang, Y.; Li, M.; Qiu, Y.; Liu, J.; Chen, J.; Xiao, Y. Graphene oxide coated Titanium Surfaces with Osteoimmunomodulatory Role to Enhance Osteogenesis. *Mater. Sci. Eng. C* **2020**, *113*, 110983. [CrossRef] [PubMed]

154. Li, Z.; Goh, T.-W.; Yam, G.H.-F.; Thompson, B.C.; Hu, H.; Setiawan, M.; Sun, W.; Riau, A.K.; Tan, D.T.; Khor, K.A.; et al. A sintered graphene/titania material as a synthetic keratoprosthesis skirt for end-stage corneal disorders. *Acta Biomater.* **2019**, *94*, 585–596. [CrossRef] [PubMed]

155. Kumar, S.; Chatterjee, K. Comprehensive review on the use of graphene-based substrates for regenerative medicine and biomedical devices. *ACS Appl. Mater. Interfaces* **2016**, *8*, 26431–26457. [CrossRef] [PubMed]

156. Ding, X.; Liu, H.; Fan, Y. Graphene-based materials in regenerative medicine. *Adv. Healthc. Mater.* **2015**, *4*, 1451–1468. [CrossRef] [PubMed]

157. Morçimen, Z.G.; Taşdemir, Ş.; Erdem, Ç.; Güneş, F.; Şendemir, A. Investigation of the Adherence and Proliferation Characteristics of SH-SY5Y Neuron Model Cells on Graphene Foam Surfaces. *Mater. Today Proc.* **2019**, *19*, 40–46. [CrossRef]

158. Feng, Z.-Q.; Shi, C.; Zhao, B.; Wang, T. Magnetic electrospun short nanofibers wrapped graphene oxide as a promising biomaterials for guiding cellular behavior. *Mater. Sci. Eng. C* **2017**, *81*, 314–320. [CrossRef]

159. Agarwal, G.; Kumar, N.; Srivastava, A. Highly elastic, electroconductive, immunomodulatory graphene crosslinked collagen cryogel for spinal cord regeneration. *Mater. Sci. Eng. C* **2021**, *118*, 111518. [CrossRef]

160. Sekuła-Stryjewska, M.; Noga, S.; Dźwigońska, M.; Adamczyk, E.; Karnas, E.; Jagiełło, J.; Szkaradek, A.; Chytrosz, P.; Boruczkowski, D.; Madeja, Z.; et al. Graphene-based materials enhance cardiomyogenic and angiogenic differentiation capacity of human mesenchymal stem cells in vitro—Focus on cardiac tissue regeneration. *Mater. Sci. Eng. C* **2021**, *119*, 111614. [CrossRef]

161. Zambrano-Andazol, I.; Vázquez, N.; Chacón, M.; Sánchez-Avila, R.M.; Persinal, M.; Blanco, C.; González, Z.; Menéndez, R.; Sierra, M.; Fernández-Vega, Á.; et al. Reduced graphene oxide membranes in ocular regenerative medicine. *Mater. Sci. Eng. C* **2020**, *114*, 111075. [CrossRef]

162. Lynch, C.R.; Kondiah, P.P.; Choonara, Y.E.; Du Toit, L.C.; Ally, N.; Pillay, V. Hydrogel Biomaterials for Application in Ocular Drug Delivery. *Front. Bioeng. Biotechnol.* **2020**, *8*, 228. [CrossRef] [PubMed]

163. Ginestra, P. Manufacturing of polycaprolactone—Graphene fibers for nerve tissue engineering. *J. Mech. Behav. Biomed. Mater.* **2019**, *100*, 103387. [CrossRef] [PubMed]

164. Polo, Y.; Luzuriaga, J.; Iturri, J.; Irastorza, I.; Toca-Herrera, J.L.; Ibarretxe, G.; Unda, F.; Sarasua, J.-R.; Pineda, J.R.; Larrañaga, A. Nanostructured scaffolds based on bioresorbable polymers and graphene oxide induce the aligned migration and accelerate the neuronal differentiation of neural stem cells. *Nanomed. Nanotechnol. Biol. Med.* **2021**, *31*, 102314. [CrossRef] [PubMed]

165. Park, J.; Choi, J.H.; Kim, S.; Jang, I.; Jeong, S.; Lee, J.Y. Micropatterned conductive hydrogels as multifunctional muscle-mimicking biomaterials: Graphene-incorporated hydrogels directly patterned with femtosecond laser ablation. *Acta Biomater.* **2019**, *97*, 141–153. [CrossRef] [PubMed]

166. Techaniyom, P.; Tanurat, P.; Sirivisoot, S. Osteoblast differentiation and gene expression analysis on anodized titanium samples coated with graphene oxide. *Appl. Surf. Sci.* **2020**, *526*, 146646. [CrossRef]

167. Bacon, M.; Bradley, S.J.; Nann, T. Graphene quantum dots. *Part. Part. Syst. Charact.* **2014**, *31*, 415–428. [CrossRef]

168. Kasouni, A.; Chatzimitakos, T.; Stalikas, C. Bioimaging applications of carbon nanodots: A review. *C J. Carbon Res.* **2019**, *5*, 19. [CrossRef]

169. Tian, P.; Tang, L.; Teng, K.S.; Lau, S.P. Graphene quantum dots from chemistry to applications. *Mater. Today Chem.* **2018**, *10*, 221–258. [CrossRef]
170. Peng, J.; Gao, W.; Gupta, B.K.; Liu, Z.; Romero-Aburto, R.; Ge, L.; Song, L.; Alemany, L.B.; Zhan, X.; Gao, G. Graphene quantum dots derived from carbon fibers. *Nano Lett.* **2012**, *12*, 844–849. [CrossRef]
171. Ye, R.; Xiang, C.; Lin, J.; Peng, Z.; Huang, K.; Yan, Z.; Cook, N.P.; Samuel, E.L.; Hwang, C.-C.; Ruan, G. Coal as an abundant source of graphene quantum dots. *Nat. Commun.* **2013**, *4*, 1–7. [CrossRef]
172. Maiti, S.; Kundu, S.; Roy, C.N.; Das, T.K.; Saha, A. Synthesis of excitation independent highly luminescent graphene quantum dots through perchloric acid oxidation. *Langmuir* **2017**, *33*, 14634–14642. [CrossRef] [PubMed]
173. Shen, J.; Zhu, Y.; Yang, X.; Zong, J.; Zhang, J.; Li, C. One-pot hydrothermal synthesis of graphene quantum dots surface-passivated by polyethylene glycol and their photoelectric conversion under near-infrared light. *New J. Chem.* **2012**, *36*, 97–101. [CrossRef]
174. Xu, M.; Li, Z.; Zhu, X.; Hu, N.; Wei, H.; Yang, Z.; Zhang, Y. Hydrothermal/Solvothermal Synthesis of Graphene Quantum Dots and Their Biological Applications. *Nano Biomed. Eng.* **2013**, *5*, 65–71. [CrossRef]
175. Li, L.L.; Ji, J.; Fei, R.; Wang, C.Z.; Lu, Q.; Zhang, J.R.; Jiang, L.P.; Zhu, J.J. A facile microwave avenue to electrochemiluminescent two-color graphene quantum dots. *Adv. Funct. Mater.* **2012**, *22*, 2971–2979. [CrossRef]
176. Zhuo, S.; Shao, M.; Lee, S.-T. Upconversion and downconversion fluorescent graphene quantum dots: Ultrasonic preparation and photocatalysis. *ACS Nano* **2012**, *6*, 1059–1064. [CrossRef]
177. Li, Y.; Hu, Y.; Zhao, Y.; Shi, G.; Deng, L.; Hou, Y.; Qu, L. An electrochemical avenue to green-luminescent graphene quantum dots as potential electron-acceptors for photovoltaics. *Adv. Mater.* **2011**, *23*, 776–780. [CrossRef]
178. Pan, D.; Zhang, J.; Li, Z.; Wu, M. Hydrothermal route for cutting graphene sheets into blue-luminescent graphene quantum dots. *Adv. Mater.* **2010**, *22*, 734–738. [CrossRef]
179. Li, F.; Lin, L.; Chen, X. Fluorescent Graphene Quantum Dots for the Determination of Metal Ions. In *Novel Nanomaterials for Biomedical, Environmental and Energy Applications*; Elsevier: Amsterdam, The Netherlands, 2019; pp. 215–239.
180. Mintz, K.J.; Bartoli, M.; Rovere, M.; Zhou, Y.; Hettiarachchi, S.D.; Paudyal, S.; Chen, J.; Domena, J.B.; Liyanage, P.Y.; Sampson, R.; et al. A deep investigation into the structure of carbon dots. *Carbon* **2021**, *173*, 433–447. [CrossRef]
181. Ritter, K.A.; Lyding, J.W. The influence of edge structure on the electronic properties of graphene quantum dots and nanoribbons. *Nat. Mater.* **2009**, *8*, 235–242. [CrossRef]
182. Zhu, S.; Song, Y.; Zhao, X.; Shao, J.; Zhang, J.; Yang, B. The photoluminescence mechanism in carbon dots (graphene quantum dots, carbon nanodots, and polymer dots): Current state and future perspective. *Nano Res.* **2015**, *8*, 355–381. [CrossRef]
183. Feng, J.; Dong, H.; Pang, B.; Shao, F.; Zhang, C.; Yu, L.; Dong, L. Theoretical study on the optical and electronic properties of graphene quantum dots doped with heteroatoms. *Phys. Chem. Chem. Phys.* **2018**, *20*, 15244–15252. [CrossRef] [PubMed]
184. Huang, H.; Liao, L.; Xu, X.; Zou, M.; Liu, F.; Li, N. The electron-transfer based interaction between transition metal ions and photoluminescent graphene quantum dots (GQDs): A platform for metal ion sensing. *Talanta* **2013**, *117*, 152–157. [CrossRef] [PubMed]
185. Shang, W.; Zhang, X.; Zhang, M.; Fan, Z.; Sun, Y.; Han, M.; Fan, L. The uptake mechanism and biocompatibility of graphene quantum dots with human neural stem cells. *Nanoscale* **2014**, *6*, 5799–5806. [CrossRef] [PubMed]
186. Gao, T.; Wang, X.; Yang, L.-Y.; He, H.; Ba, X.-X.; Zhao, J.; Jiang, F.-L.; Liu, Y. Red, yellow, and blue luminescence by graphene quantum dots: Syntheses, mechanism, and cellular imaging. *ACS Appl. Mater. Interfaces* **2017**, *9*, 24846–24856. [CrossRef]
187. Campuzano, S.; Yáñez-Sedeño, P.; Pingarrón, J.M. Carbon dots and graphene quantum dots in electrochemical biosensing. *Nanomaterials* **2019**, *9*, 634. [CrossRef]
188. Iannazzo, D.; Pistone, A.; Salamò, M.; Galvagno, S.; Romeo, R.; Giofré, S.V.; Branca, C.; Visalli, G.; Di Pietro, A. Graphene quantum dots for cancer targeted drug delivery. *Int. J. Pharm.* **2017**, *518*, 185–192. [CrossRef]
189. Li, D.; Na, X.; Wang, H.; Wang, C.; Yuan, Z.; Zhu, B.-W.; Tan, M. The effects of carbon dots produced by the Maillard reaction on the HepG2 cell substance and energy metabolism. *Food Funct.* **2020**, *11*, 6487–6495. [CrossRef]